Biased random walk in energetically disordered lattices

Issak Avramov and Andrey Milchev
Institute for Physical Chemistry, Bulgarian Academy of Sciences, G. Bonchev Str. Block 11, 1113 Sofia, Bulgaria

Eleni Arapaki and Panos Argyrakis
Department of Physics, University of Thessaloniki, 54006 Thessaloniki, Greece
(Received 12 January 1998)

We utilize our previously reported model of energetically disordered lattices to study diffusion properties, where we now add the effect of a directional bias in the motion. We show how this leads to ballistic motion at low temperatures, but crosses over to normal diffusion with increasing temperature. This effect is in addition to the previously observed subdiffusional motion at early times, which is also observed here, and also crosses over to normal diffusion at long times. The interplay between these factors of the two crossover points is examined here in detail. The pertinent scaling laws are given for the crossover times. Finally, we deal with the case of the frequency dependent bias, which alternates (switches) its direction with a given frequency, resulting in a different type of scaling. [S1063-651X(98)11008-5]

PACS number(s): 05.40.+j, 05.60.+w

I. INTRODUCTION

Diffusion in the presence of disorder is an ever enlarging field due to a wealth of new phenomena and processes that are being unravelled [1,2]. While the mechanism for the diffusion process itself is rather simple, in the presence of disorder it is much more difficult to treat because one now has a combination of two stochastic processes, strongly dependent on each other. The details of their coupling is not clear, but one must take into account the fact that disorder can appear in a wide variety of different forms: it can be deterministic or (statistically) random, geometric or energetic, constant or varying with time, etc. so that the emerging system is a combination of several different factors, each one of which must be properly treated in a separate way. The main expectation is that the transport properties behave irregularly, leading to highly anomalous diffusion of classical particles. The disorder itself can be geometric, due to an irregular lattice structure, such as, for example, the percolation model or a variety of fractal structures, in which case the details are determined by the ramifying characteristics present. Or it can be energetic, in which case the lattice sites (or bonds) are assigned different energy states. We have recently introduced a model [3–6] with the latter type of disorder, which is placed on the bonds between the sites. The difference between site and bond disorder was pointed out in the past [1], and it affects the symmetry of the transition probabilities between adjacent sites. Our model assigns a different energy E to every lattice bond, so that a particle hopping from one site to the next has to overcome a potential barrier. The extent of disorder can be varied using a dispersion parameter [7]. Transitions are performed by a hopping mechanism which is now very common in treating disordered systems with a large variety of applications, such as in semiconductor systems, in ionic conductivity, in superionic solids, in carrier recombination in glasses, and in dispersion in flow through porous media. Modified random walk models that take the disorder into account are also used in such approaches.

A general behavior characterizing these systems is that disorder results in anomalous diffusion laws. It slows down the diffusion process at early times. However, there exists a crossover time τ_c, after which diffusion becomes normal with time. In a sense this crossover time is the characteristic ''equilibration'' time, the time it takes for the diffusing particles to reach an ''equilibrium'' state with the underlying disorder. This point has been also compared in the past with the percolation picture, in which the crossover time is a strong function of the temperature T. Thus τ_c gives the onset of the exploitation of open channels for the particle to diffuse, as a function of the order parameter T. The Arrhenius plot of τ_c vs $1/T$ indeed produces identically the critical threshold value, for two- and three-dimensional lattices [3]. This trend of early t anomaly / long t linearity is not unique in our system. There is a plethora of different systems where equivalent behavior is observed. To name a few: adsorption and diffusion of interacting particles on a surface [8], and diffusion on extremely rugged energy landscapes with equal minima [9,10].

Nonsymmetric diffusion has in the past also been a pertinent model for understanding several processes, such as, for example, the excitonic motion at low temperatures [11], hydrogen diffusion in group-VB metals at higher temperatures [12], the creation of vacancies in solids [13], etc. In these works there is an abundance of theoretical and simulation results modeling the experimental data. The nonsymmetrical characteristic was due to the retention of memory of the previous steps, resulting in enhanced diffusion. In the present work we also use asymmetric diffusion, which is now due to one designated preferred direction, constant in space and time, resulting in a drift-type motion, resembling the presense of an external field. This also results in superlinear behavior. This type of motion is amenable to oriented systems, such as columnar liquid crystals, or kinetics in electrophoresis. Technically, this is done by lowering the energy barriers in a preferred direction, while raising the equivalent in the opposite direction for the duration of the hop. This is done by adding (subtracting) a bias factor ϵ to (from) the

 © 1998 The American Physical Society

values of the energy barriers along (opposite to) the bias direction. A ballistic type of motion is expected, and is indeed observed. The overall system behavior depends on the interplay of ϵ, and the temperature.

A new picture emerges if the bias factor is not constant in time, but varies with a given frequency ω. It is a picture of ''alternating current,'' with the electrons switching direction every $1/\omega$ steps. This also results in superlinear behavior of the mean-square displacement. Frequency dependent diffusion has been studied in the past [14–16], but there the mechanism involves the entire renewal of the disorder details every $1/\omega$ steps, while in the present model the disorder is frozen and only the bias direction is frequency dependent.

II. MODEL

We start with the earlier described [3–6] Monte Carlo model, according to which a square lattice is generated in a way that each two neighboring sites are connected with a channel (bond) having an energy barrier with a height that is generated randomly from a given distribution. The height of the barriers depends on the average value $\langle E\rangle$, and on a given dispersion parameter σ, in the following way:

$$E_{ij}=\langle E\rangle-\sigma(x-0.5), \tag{1}$$

where x is a random number between 0 and 1 from a given distribution (say, a uniform random number distribution). The parameter σ shows how widely dispersed the energies are distributed, with large σ values denoting a large degree of disorder, while as $\sigma\rightarrow 0$ the system becomes a perfect lattice. All barriers remain frozen during the entire process. Thus this model resembles the model of a rugged energy landscape, where the ruggedness (σ) can be varied at will [7]. A particle is placed at a random position (site) on the lattice, and then performs random walks. The decision whether to jump or stay still and to what direction is based on the local environment and follows the Boltzmann statistics. The probabilities P_{ij} to jump from site i to site j are calculated by:

$$P_{ij}=\frac{1}{z}\,\exp(-E_{ij}/kT). \tag{2}$$

Here z is the coordination number, k the Boltzmann constant, and T the system temperature. For convenience we take $k=1$, and the temperature is measured in energy units. There is also a finite probability to remain on the same site (no jump), which is given by

$$P_{ii}=1-\sum_{j\neq i} P_{ij}\,. \tag{3}$$

The present barrier model has the feature that at all times $P_{ij}=P_{ji}$, since randomness is incorporated into the lattice bonds and not into the lattice sites. For the latter model this is not the case. We now introduce a bias parameter ϵ, only in one of two dimensions, say in the y dimension. This factor makes jumps in one direction of the y axis somewhat easier (more probable), and jumps in the opposite direction of the same axis more difficult. This is done by momentarily lowering the height of the barrier along the direction of bias by a fixed amount, $(\langle E\rangle/2)\,\epsilon$, and increasing the barriers in the opposite direction by the same amount. Thus the energy barriers for the motion along the bias dimension become

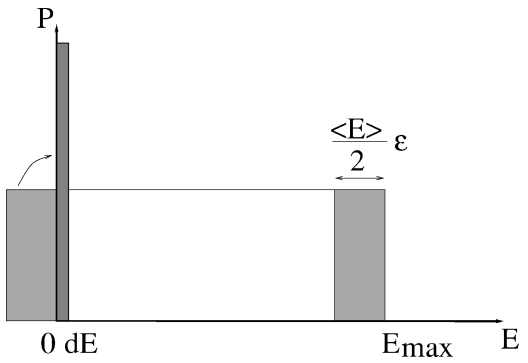

FIG. 1. The effective new distribution of energies after the inclusion of the bias factor ϵ. This factor has as a result the lowering of the $E_{\max}$ value by the ammount of $(\langle E\rangle/2)\,\epsilon$, as shown.

$$E_{ij}^{(y)}=\langle E\rangle_y-\sigma_y(x-0.5)\mp\frac{\epsilon}{2}\langle E\rangle_y\,. \tag{4}$$

The parameter ϵ can take any positive value, and thus the term $(\langle E\rangle/2)\,\epsilon$ represents a multiple (or fraction) of $\frac{1}{2}$ the average energy value. This lowering/raising is not permanent, but is considered to occur only for the duration of a single jump, while the barrier energies revert to their regular values afterwards. The minus sign pertains for the motion along the direction of bias, while the plus sign for the opposite direction. Since negative values of $E_{ij}^{(y)}$ are not permitted, $E_{ij}^{(y)}$ is set equal to zero ($E_{ij}^{(y)}=0$) in all cases when negative values are obtained according to Eq. (4). A schematic of the modified density distribution is given in Fig. 1, where we observe the shift of the right boundary toward the left by the amount $(\langle E\rangle/2)\,\epsilon$. This results in a corresponding part with negative energies E, in the left boundary, which is moved and added to a δ function on zero.

The dimension that contains no bias is not affected at all, and, thus, the forward and backward jumps in the x dimension (the dimension perpendicular to the bias) have the same probability as before. In this way the barrier (bond) energies in the x dimension are defined by an expression similar to Eq. (1):

$$E_{ij}^{(x)}=\langle E\rangle_x-\sigma_x(x-0.5). \tag{5}$$

The result of such a biased walk is schematically shown in Fig. 2, where we give two typical walks, starting at the same point on the lattice: one with no bias and one with bias. The case with no bias results in a regular random walk motion, similar in nature to a random walk on a regular surface. The details of the energy barriers do not show at all, and do not affect the path traveled by the particle. For the case with bias we clearly see the directional character of the motion. We observe a path that is almost unidirectional, along the direction of the bias. In this pictorial the lattice size is 400 $\times$1000; the random walk starts at the midpoint, i.e., at (200, 500); the end point is around (200, 570). This is because the bias makes the particle to preferentially move toward the right in the lattice.

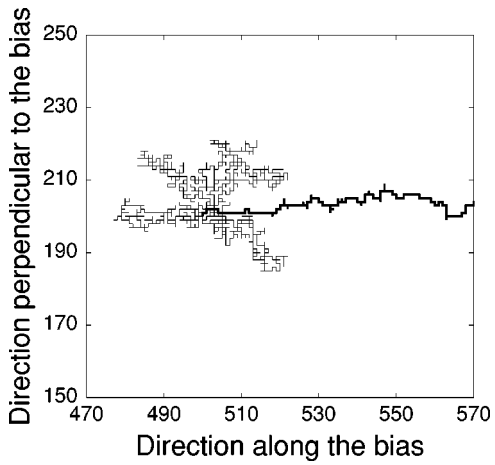

FIG. 2. Pictorial of the path of a particle in the case of normal diffusion with no bias (thin line), and the case of diffusion with a bias of $\epsilon=0.9$ (thick line). The temperature here is $T=0.075$. The direction of the bias in this case is along increasing x values. Both walks start at the same origin, which is here (500,200).

The mean values of the energy barriers along the x and y dimensions, $\langle E\rangle_x$ and $\langle E\rangle_y$, and the corresponding dispersion parameters σ_x and σ_y, can be varied at will. This allows one to model the motion in more or less oriented systems, or systems with anisotropic characteristics. For instance, one-dimensional motion is obtained for $\langle E\rangle_x \gg \langle E\rangle_y$ and $\sigma_x=0$. Therefore, the algorithm permits one to have an asymmetric motion in two dimensions, not only due to the bias but also when $\langle E\rangle_x \neq \langle E\rangle_y$, or $\sigma_x \neq \sigma_y$. The problem can be easily extended to three dimensions, using the same ideas and model discussed above.

In a further development, the sign of the direction of the bias can alternate in time with a given frequency ω. In this case the sign of the strength of ϵ is changing after $1/\omega$ steps, but always along the same coordinate. In this way the energy barriers for a motion along the bias dimension become:

$$E_{ij}^{(y)}=\langle E\rangle_y-\sigma_y(x-0.5)\mp\frac{\epsilon(\omega)}{2}\langle E\rangle_y. \tag{6}$$

III. SIMULATION PARAMETERS

Here we give the parameter values used in the Monte Carlo calculations. Typical sizes for the square lattice used here have lengths of 1000×400 sites. The reason we use a rectangle, rather than a square, is because the displacement along the coordinate with the bias is always larger than the one with no bias. Particles are placed in the center of the lattice before the walk is started. We always use cyclic boundary conditions. In all computations we use a uniform random number distribution, and we set $\langle E\rangle_x=\langle E\rangle_y=0.5$ and $\sigma_x=\sigma_y=1$. This means that we have the maximum width of energies in the range between 0 and 1, in both dimensions. The bias parameter ϵ is varied between $0<\epsilon<5.0$. The temperature T is in the range $0.05<T<1000$. The frequency ω changing the bias direction is in the range $10^{-4}<\omega<1$. Typical times sampled are up to 1×10^6 steps (exceptionally, at low temperatures we reach 10×10^6 steps).

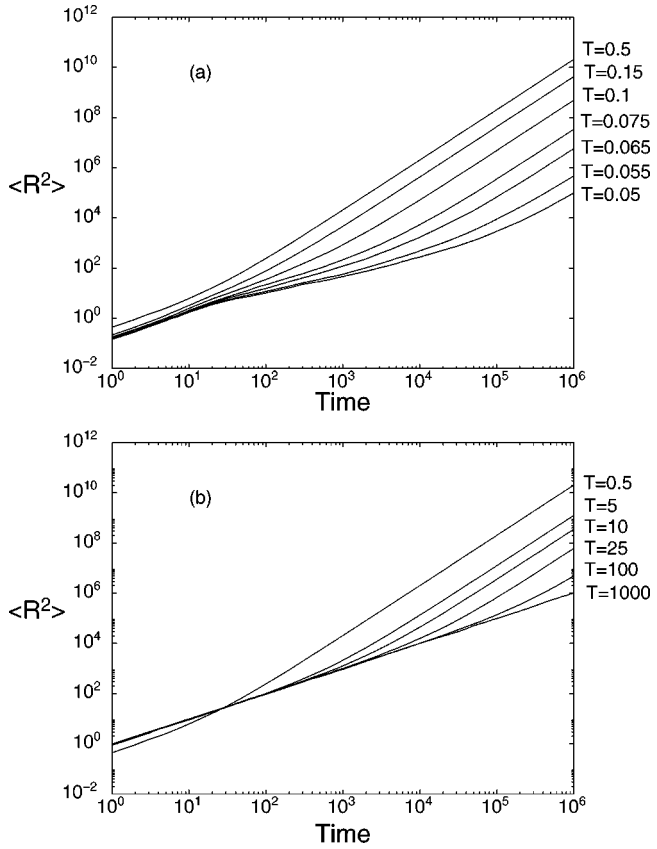

FIG. 3. The mean-square displacement $\langle R^2\rangle$ as a function of time (number of steps), for several different temperatures $T=0.05$, 0.055, 0.065, 0.075, 0.1, 0.15, and 0.5 (a), and $T=0.5$, 5, 10, 25, 100, and 1000 (b), for a frozen 2D lattice of size 400×1000, in log-log form. The bias parameter $\epsilon=1.8$ and the dispersion $\sigma=1.0$. We used 1000 realizations.

IV. RESULTS AND DISCUSSION

A. Unidirectional biased random walk

In Fig. 3, we plot the mean-square displacement $\langle R^2\rangle$, as a function of time for a fixed value of the bias parameter $\epsilon=1.8$, and several different temperatures, in the range $T=0.05$–1000. Because of different trends present, we show this figure in two parts: (a) low T and (b) high T. We observe in part (a), where T is in the range $T=0.05$–0.5, that in the long time limit all slopes reach a limiting value of 2, which is the expected result, since this model represents a form of ballistic motion whereby in the presence of external field (bias) the particle drifts with a constant velocity along the field, so that $\langle R^2\rangle\sim t^2$. The time it takes to reach this limiting value is a strong function of temperature. The lower the temperature, the longer this takes. Ignoring the first ten steps, at early times we observe that the system is subdiffusive, which is more pronounced the lower the temperature. The reason for this behavior is the same as observed for the simple case of no bias reported earlier by us [3–5]. The particle is trapped in some region of space which forms a low-lying valley, and it must overcome some activation energy barriers, given by the barrier heights of the model. This can happen only via a thermal mechanism, so at very low temperatures detrapping from such a low-lying valley is highly unlikely, and the particles spend a considerable

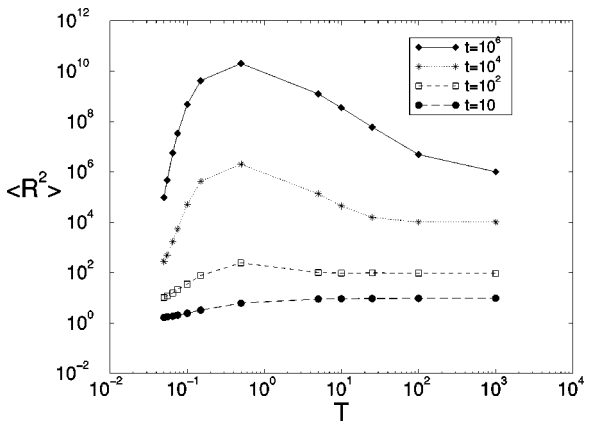

FIG. 4. The mean-square displacement $\langle R^2 \rangle$ as a function of temperature T, for the same data of Fig. 3, for $\epsilon = 1.8$.

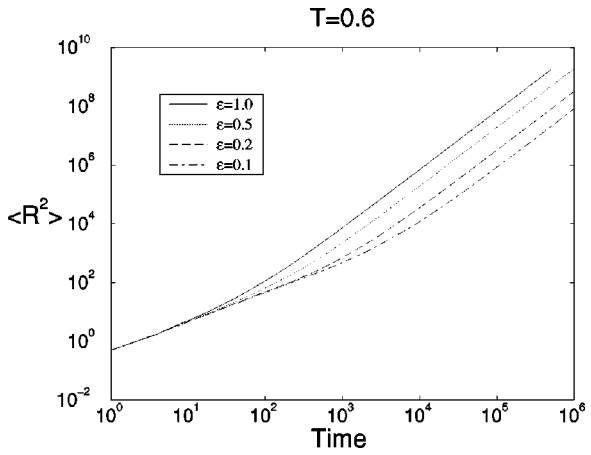

FIG. 5. The mean-square displacement $\langle R^2 \rangle$ as a function of time (number of steps), for several different values of the bias ϵ, $\epsilon = 0.1$, 0.2, 0.5 and 1.0, for a frozen 2D lattice of size 400 $\times$1000, in log-log form. The temperature is $T = 0.6$ and the dispersion $\sigma = 1.0$ (1000 realizations).

amount of time before making a successful jump over a high barrier. Eventually, at long t, a limiting slope of 2 is always attained, and the system is again in an ''equilibrium'' state. This happens for any value of $\epsilon \neq 0$. Naturally, the smaller the ϵ value, the longer it takes for this to happen. We thus choose for Fig. 3 a relatively large value ($\epsilon = 1.8$) to speed up this effect.

In Fig. 3(b), we show the range $T = 0.5$–1000. Here we observe an opposite effect to that shown in Fig. 3(a), i.e., $\langle R^2 \rangle$ decreases with increasing temperature. More importantly, the limiting slope of 2 progressively changes to a limiting value of 1, which is fully attained at the highest temperature $T = 1000$. This happens because, as the temperature is progressively increased, there is enough thermal energy to overcome barriers of any height, so that the effect of bias (which results in simultaneous increasing and decreasing of two barriers along one direction) is not that important anymore. At $T = \infty$ the slope of the $\langle R^2 \rangle$ line would be exactly equal to 1, since the effect of the bias is completely lost. Had we combined parts (a) and (b) in Fig. 3, several curves would necessarily cross. The effect is shown more clearly in Fig. 4, where we plot $\langle R^2 \rangle$ vs T for several fixed times. We observe in all cases that there is a maximum around $T = 0.5$. This is the crossover point where the combination of the two opposite trends produces the largest $\langle R^2 \rangle$ value. In Fig. 4 we plot $\langle R^2 \rangle$ vs T for several fixed times t, $t = 10$, 10^2, 10^4, and 10^6 steps. We see that the maximum (optimum) value is always around $T = 0.5$, while this maximum is more pronounced at longer times.

The effect of the bias ϵ is shown by the data of Table I, where we show the fraction $\langle R_x^2 \rangle / \langle R_y^2 \rangle$, the bias being along the y axis. All trends are as expected, i.e., the fraction decreases with increasing ϵ for low and intermediate T, while it is almost constant for very high T.

In Fig. 5, we plot $\langle R^2 \rangle$ as a function of time, for a constant temperature ($T = 0.60$), which is in the intermediate T range, for several different values of the bias parameter ϵ. We observe the expected peel-off effect, i.e., the smaller the ϵ value the longer it takes for the system to acquire the ballistic character. Eventually all slopes reach the limiting value of 2, as expected, since at this temperature the effect of the bias is important.

For all curves of Figs. 3 and 5, the time it takes to reach this limiting slope, τ_c, strongly depends on the system temperature T and bias factor ϵ, respectively. For the data of Fig. 3(a), for high temperatures ($T = 0.5$) this happens relatively early, but as the temperature is decreased ($T = 0.05$), τ_c gets progressively longer. This behavior is analogous to our earlier result [3] for the case of no bias ($\epsilon = 0$), in which case the curves and trends are similar, but the limiting slope was the classically expected slope of 1.0, resulting in a typical Arrhenius behavior. However, in that case the R^2 data were monotonic with temperature, while here this is not the case. If we still prepare such a plot, we see in Fig. 6 that

TABLE I. The ratio of the mean-square displacement perpendicular to the bias, $\langle R_x^2 \rangle$, over the mean-square displacement along the bias, $\langle R_y^2 \rangle$, for various values of bias and temperature, at a fixed time ($t = 10^6$ MC steps). We used 500 realizations.

ϵ	$\frac{\langle R_x^2 \rangle}{\langle R_y^2 \rangle}$ ($T=0.075$)	$\frac{\langle R_x^2 \rangle}{\langle R_y^2 \rangle}$ ($T=0.15$)	$\frac{\langle R_x^2 \rangle}{\langle R_y^2 \rangle}$ ($T=0.5$)	$\frac{\langle R_x^2 \rangle}{\langle R_y^2 \rangle}$ ($T=5$)	$\frac{\langle R_x^2 \rangle}{\langle R_y^2 \rangle}$ ($T=1000$)
0.1	0.01928	0.00223	0.00214	0.0821	0.9726
0.3	0.00526	0.0003	0.000265	0.0097	0.9744
0.5	0.00319	0.00011	0.0000954	0.0037	0.9658
0.7	0.00177	0.00006	0.00005127	0.0020	0.9579
0.9	0.000897	0.00004394	0.00003356	0.0012	0.9478

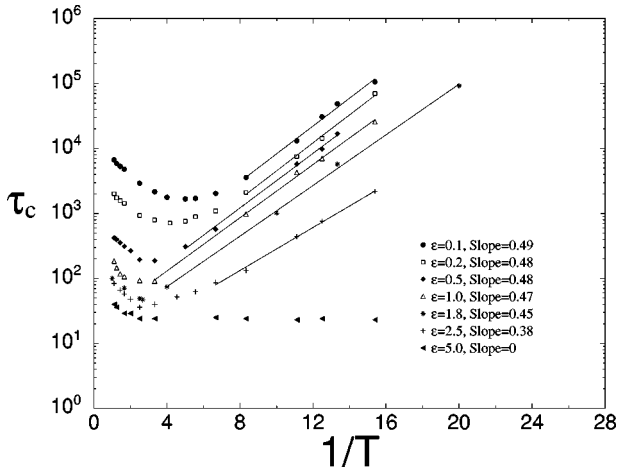

FIG. 6. The crossover time τ_c (the time after which $\langle R^2 \rangle$ becomes linear), as a function of $1/T$ for the same data as in Fig. 3 ($\epsilon = 1.8$), and several more ϵ values.

below a certain temperature ($T < 0.50$) we obtain straight lines for all cases, i.e., we have Arrhenius behavior at the entire range. Above $T > 0.50$ we do not obtain Arrhenius behavior due to the thermal effect discussed above. The τ_c values that were used in this figure were derived as the cross point of the two straight line segments (early time and late time) of each curve of Fig. 3. The best fits from linear least squares were used in each case. The first and last points needed to calculate the fit were chosen arbitrarily, by optically estimating the departure from linear behavior. In Fig. 6 we have also included several additional ϵ values. In Table II we give the slopes of the straight lines for all these cases. For $\epsilon = 0$ we obtain a slope of approximately 0.5, which was explained in the past to conform with the percolation picture, since $p_c = 0.50$ is the critical percolation threshold for bond percolation in two dimensions. Then, for different ϵ values, we obtain slopes that are progressively smaller than 0.5. The difference from 0.5 is proportional to ϵ, i.e., the larger the bias the more different is the crossover value from the 0.50 value.

We make the assumption that the temperature dependence of τ_c, for the straight line section of these curves, follows an experimental law

$$\tau_c = \exp\left(\frac{E_{\text{eff}}}{kT}\right). \tag{7}$$

TABLE II. The slopes of the straight lines of the Arrhenius plots of the crossover times t_c, for several biases investigated in Fig. 5.

ϵ	Slope of t_c
0	0.508
0.1	0.49
0.2	0.476
0.5	0.48
1.0	0.471
1.8	0.449
2.5	0.38
5.0	0

In the case of no bias, this leads to the picture [3] of the availability of open channels through which the particle can propagate. Even though here we do not have a binary lattice of open and closed bonds, still it was shown [3] that this problem corresponds to an effective percolation problem, for which one should define and/or find the critical threshold value by monitoring diffusion in a wide temperature range. This produced a critical value of $p_c = 0.5$, from the Arrhenius plot data, similar to Fig. 6. In our new problem here the inclusion of the bias ϵ effectively decreases E_{eff}. The lowering of E_{eff} with increasing bias can be explained by taking into account at least two additional effects: First, with the increase of bias the dimensionality of the motion is changing from two dimensional (for $\epsilon = 0$) to quasi-one-dimensional (for $\epsilon = \infty$); a good illustration of this effect was shown in Fig. 2. Therefore, the effective p_c now depends on ϵ. Second, the position of E_{eff} is determined [17,18] by the equation

$$\int_0^{E_{\text{eff}}(\epsilon)} P(E)dE = p_c(\epsilon), \tag{8}$$

where $P(E)$ is the spectrum (the probability distribution function of the barrier heights), with the limiting condition

$$\int_0^{E_{\max}(\epsilon)} P(E)dE = 1. \tag{9}$$

In the case of no bias ($\epsilon = 0$), we have a uniform distribution of energy barriers $P(E) = P$, and the upper limit of the integral in Eq. (9) is

$$E_{\max} = 2\langle E \rangle, \tag{10}$$

so that

$$P = \frac{1}{E_{\max}}. \tag{11}$$

In the case of finite bias ($\epsilon > 0$), it is useful to split the integral in the following way:

$$\int_0^{E_{\text{eff}}(\epsilon)} P(E)dE = \int_0^{\Delta E} P(E)dE + \int_{\Delta E}^{E_{\text{eff}}(\epsilon)} P(E)dE. \tag{12}$$

As we reduce every barrier along the bias axis by the amount $(\langle E \rangle/2)\,\epsilon$, the probability distribution function remains uniform. Only in the $P(E)$ versus E plot must the rectangle be shifted to the left for a distance $(\langle E \rangle/2)\,\epsilon$, as shown in Fig. 1. This means that $P = 0$ above the quantity $[E_{\max} - (\langle E \rangle/2)\,\epsilon]$, while it remains $P = 1/(2\langle E \rangle)$ (unchanged) below this limit. Then we set all negative energies exactly at zero. This means that $P(E)$ is changed, but only in the vicinity of $E = 0$, and it is changed in such a way that the first integral is becoming $P(\langle E \rangle/2)\,\epsilon$, while in the interval between dE and $[2\langle E \rangle - (\langle E \rangle/2)\,\epsilon]$ the probability is again P.

By taking into acount the explicit form of $P(E)$, one has

$$E_{\text{eff}} = 2\langle E \rangle p_c(\epsilon) - \frac{\langle E \rangle}{2}\epsilon, \tag{13}$$

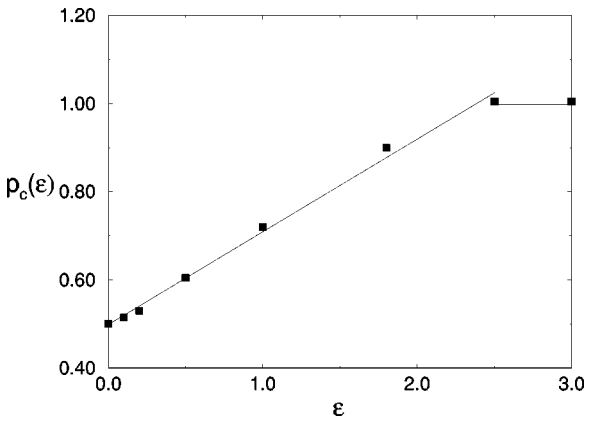

FIG. 7. The percolation threshold $p_c(\epsilon)$ vs ϵ. The straight line is the best linear fit with slope 0.21.

where the critical threshold is a function of the bias factor ϵ. From Eq. (7), it follows that the slopes of $\ln(\tau_c)$ versus the $1/T$ plot, given in Fig. 6 (and listed in Table II), are equal to $E_{\text{eff}}(\epsilon)$ (in k units). Thus, we can use these data to determine from Eq. (13) the dependence of the percolation threshold p_c on ϵ. At this point there is no basis for any predictions for this dependence. Our results are shown in Fig. 7. It is seen that p_c grows linearly from 0.5 (for $\epsilon=0$, two-dimensional motion) to 1 (for $\epsilon=2.2$, quasi-one-dimensional motion). The best fit for the straight line gives a relationship

$$p_c = 0.5 + 0.225\epsilon. \tag{14}$$

We conclude that the inclusion of the bias in the motion has as a result the linear increase of the value of the threshold, p_c, making the motion one-dimensional-like. We also observe that the value $\epsilon=2.2$ produces a p_c value of $p_c=1$, which is the upper limit. This effectively says that for this value the motion is one dimensional. This is not a generalized result, since it comes from simulations using the particular energy distributions, dispersion σ, etc.

In Fig. 8 we plot in log-log coordinates the critical temperarure T_c above which the mechanism of motion switches from ballistic motion to random walk against the bias ϵ. T_c

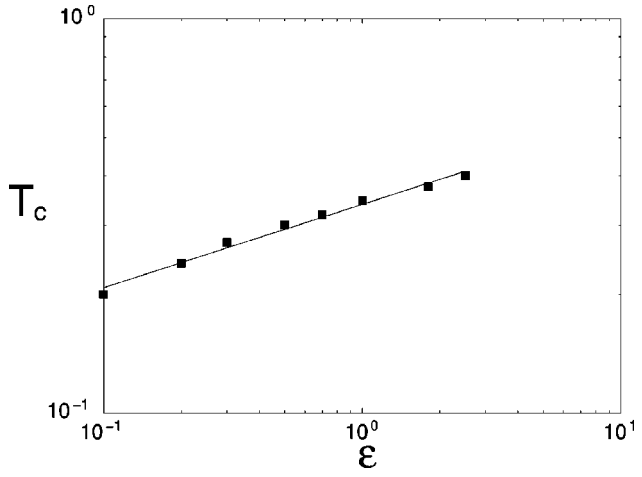

FIG. 8. Plot of the critical temperature T_c vs ϵ from the data of Fig. 6.

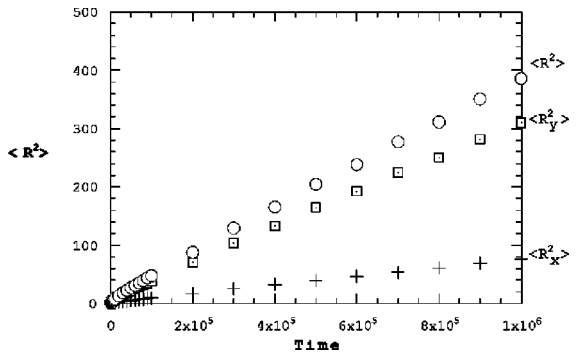

FIG. 9. The mean-square displacement as a function of time for a fixed frequency $\omega=0.1$. Both the x and y components of $\langle R^2\rangle$ are plotted.

is given by the temperature at which a minimum appears in the τ_c against $1/T$ curves in Fig. 6. It follows that T_c scales with ϵ as $T_c \sim \epsilon^{0.21}$.

B. Frequency dependent biased random walk

We now turn to the case of a frequency dependent bias, when $\epsilon=\epsilon(\omega)$. Figure 9 gives the behavior of the mean-square displacement $\langle R^2\rangle$ as a function of time for a frequency $\omega=0.1$. This means that every $1/\omega=10$ time steps the bias direction changes sign, but always on the same dimension, say the y dimension mentioned earlier. In the same figure are also given the mean-square displacements along the bias axis, $\langle R_y^2\rangle$, and perpendicular to the bias axis, $\langle R_x^2\rangle$. If the bias ϵ is constant with respect to time, then the $\langle R^2\rangle$ curve is parabolic in linear coordinates. When the bias is alternating at a given frequency, we observe an almost linear $\langle R^2\rangle$ vs time dependence. On the other hand, because of the bias $\epsilon(\omega)$, the increase of the diffusion coefficient is considerable. The results for $T=0.05$ and $\omega=0.1$ are given in Fig. 9. We have obtained similar results for $T=0.1$ and other temperatures.

The manner in which the mean-square displacement along the bias axis, $\langle R_y^2\rangle$, depends on frequency ω is illustrated in Fig. 10, for $T=0.05$. Because of the alternation of the sign of $\epsilon(\omega)$, the $\langle R_y^2\rangle$ against time dependence is sawtooth-like. This is clearly seen in the inset in the figure, for $\omega=0.0001$ (i.e., the sign is reversed each 10 000 steps). For all other frequencies only lines connecting the minima of the corresponding sawtooth-like curves are presented. The slopes of the curves are the diffusion coefficients $D_y(\omega)$ in the direction along the bias axis.

When bias is applied, the particle moves predominantly along the direction of the bias (like running downhill), while being confined within a low barrier valley, surrounded by ridges of high barriers. Thus it comes comparatively quickly to the border of the valley. Due to the bias, the bordering barriers (in the bias direction) will be lower, but the hopping particle will still need some characteristic time τ_c until the ridge is overcome and a new valley entered. Now, if the bias direction is reversed within a period $\omega^{-1}\ \langle\tau_c\rangle$, the lower ridge of barriers will again grow higher and the particle will fail to overcome them within the characteristic time τ_c. Clearly, the higher ω is, the less mobile the hopping particle will be, i.e., there is a small probability for successful move-

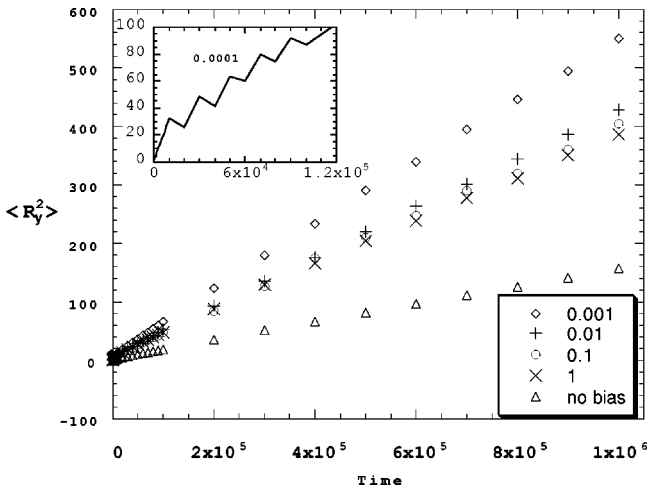

FIG. 10. The mean-square displacement $\langle R_y^2 \rangle$ as a function of time for several different frequencies ω, as designated. The inset contains the detail of the plot origin, where we observe the ''sawtooth'' behavior discussed in the text. The temperature here is $T=0.05$.

ment along the rugged landscape of the lattice. Generally, this should lead to an overall reduction of the diffusion coefficient, as shown in Fig. 11. It is of interest to explore further the dependence of D_y on the frequency ω. Since D depends strongly on the frequency, one might assume the existence of a scaling law and a possible relationship

$$D_y(\omega) \sim \omega^{-a}. \tag{15}$$

However, as the data in Fig. 11 shows, this is only a very rough approximation, since the curves, for the range of values examined, are not strictly speaking straight, but exhibit some curvature.

Several related models have recently appeared in the literature [19–22], which monitor motion in a field of a potential which is sawtooth-like, as it is the shape of the inset in Fig. 10, called ''ratchet potential.'' These potentials are typically noise induced [19,22], and it has been shown that the breaking of the spatial symmetry and time modulation result in a Brownian particle acquiring a net macroscopic motion in a specific direction [20,22], equivalent to our result of Figs. 9 and 10. These models are met in biological motor protein systems. While these processes are analogous to the behavior met in the present work, there are no properties reported like the ones we monitor, in order to make a direct comparison. Our interest has been in the behavior of the square displacement as a function of time, while in the rachet potential cases the interest is in how noise induces directional motion.

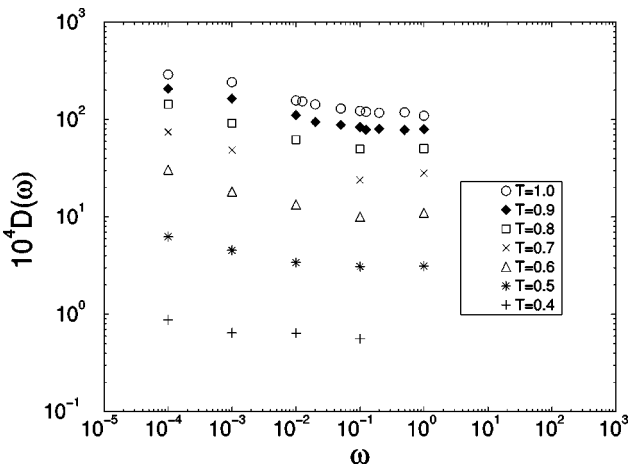

FIG. 11. The diffusion coefficient $D(\omega)$ as a function of the frequency ω of the bias, for several different temperatures.

V. CONCLUDING REMARKS

We presented a diffusion model for energetically disordered two-dimensional systems in which motion can be correlated according to an external field, and, therefore, partially acquire a one-dimensional character. This was done by incorporating a bias factor ϵ in the random walk model. The value of ϵ quantitatively determines this character. Thus, when $\epsilon=0$, we have a regular random walk, while when $\epsilon=\infty$ we have a motion along a perfect straight line, i.e., fully correlated motion. The values of ϵ in between are of interest, as the system displays a crossover from ballistic to normal diffusion, and from early time to long time. The crossover scalings have been found numerically.

Second, this model gives a picture of motion whose behavior can be controlled via two parameters, the bias ϵ and the temperature T, which can act as switches to control the dimensionality of the motion. We derived numerical equations that connect ϵ with the effective ''percolation threshold'' p_c.

Our next finding is the increase of the diffusion coefficient as soon as a bias with a frequency ω is applied. The result is not trivial, because half the time the bias accelerates the motion and half of the time impedes it. Still the net effect is a considerable increase of the diffusion coefficient.

ACKNOWLEDGMENTS

This work was supported by the Greek-Bulgarian Bilateral Scientific Cooperation, and Copernicus Project No. CIPACT930105.

[1] J. Haus and K. W. Kehr, Phys. Rep. **150**, 263 (1987).
[2] J. P. Bouchaud and A. Georges, Phys. Rep. **125**, 127 (1990).
[3] I. Avramov, A. Milchev, and P. Argyrakis, Phys. Rev. E **47**, 2303 (1993).
[4] A. Hörner, A. Milchev, and P. Argyrakis, Phys. Rev. E **52**, 3570 (1995).
[5] P. Argyrakis, A. Milchev, V. Pereyera, and K. W. Kehr, Phys. Rev. E **52**, 3623 (1995).
[6] E. Arapaki, P. Argyrakis, I. Avramov, and A. Milchev, Phys. Rev. E **56**, R29 (1997).
[7] K. Sapag, V. Pereyra, J. L. Riccardo, and G. Zgrablich, Surf. Sci. **295**, 433 (1993).

[8] I. Vattulainen, J. Merikoski, T. Ala-Nissila, and S. C. Ying, Surf. Sci. **366**, L697 (1996).
[9] J. C. Dyre, Phys. Rev. B **49**, 11 709 (1994).
[10] J. C. Dyre and J. M. Jacobsen, Phys. Rev. E **52**, 2429 (1995).
[11] P. Argyrakis and R. Kopelman, Chem. Phys. **57**, 29 (1981); **78**, 251 (1983).
[12] V. Lottner, J. W. Haus, A. Heim, and K. W. Kehr, J. Phys. Chem. Solids **40**, 557 (1979).
[13] A. Dafano and G. Jacucci, Phys. Rev. Lett. **39**, 950 (1977); J. Nucl. Mater. **69/70**, 549 (1978).
[14] S. D. Druger, A. Nitzan, and M. A. Ratner, J. Chem. Phys. **79**, 3133 (1983).
[15] S. D. Druger, M. A. Ratner, and A. Nitzan, Phys. Rev. B **31**, 3939 (1985).
[16] A. Nitzan and M. A. Ratner, J. Chem. Phys. **98**, 1765 (1994).
[17] I. Avramov and A. Milchev, J. Non-Cryst. Solids **104**, 253 (1988).
[18] I. Avramov, J. Chem. Phys. **25**, 4439 (1991).
[19] M. O. Magnasco, Phys. Rev. Lett. **71**, 1477 (1993); **72**, 2656 (1994).
[20] T. E. Dialynas, K. Lindenberg, and G. P. Tsironis, Phys. Rev. E **56**, 3976 (1997).
[21] F. Marchesoni, Phys. Rev. E **56**, 2492 (1997).
[22] L. P. Faucheux, L. S. Bourdieu, P. D. Kaplan, and A. J. Libchaber, Phys. Rev. Lett. **74**, 1504 (1995).